

Original Article

Optimized intraoperative frozen sectioning improves diagnostic quality and efficiency

Ting Huang¹, Guanping Chen²

¹Department of Pathology, Tongde Hospital of Zhejiang Province, Hangzhou, Zhejiang, China; ²Tumor Research Institute of Integrated Traditional Chinese and Western Medicine, Tongde Hospital of Zhejiang Province, Hangzhou, Zhejiang, China

Received July 10, 2025; Accepted November 23, 2025; Epub December 15, 2025; Published December 30, 2025

Abstract: Objectives: This study aimed to optimize traditional frozen section (FS) methods through tissue-specific modifications to enhance section quality, reduce diagnostic time, and improve diagnostic clarity. Methods: Comparative analysis was performed on three tissue types: cavity-rich pulmonary tissue, adipose-rich lymph nodes, and calcified thyroid specimens. Using conventional versus optimized FS protocols, with improvements assessed via section integrity, flatness, knife mark frequency, and Hematoxylin and eosin (H&E) staining quality. For cavity-rich pulmonary tissue, a thin adhesive layer was applied to completely encapsulate the tissue surface, followed by immediate cryocompression using the freezing hammer. For adipose-rich lymph nodes, each sample head should ideally contain a single lymph node, while addressing sectioning direction, and avoiding excessively low temperatures. For calcified thyroid specimens, increased sectioning speed through rapid handle rotation achieved swift tissue cutting, while consistent speed exacerbates tissue folding. Results: Following protocol optimization, cavity-rich pulmonary tissue demonstrated improved integrity with well-preserved alveolar architecture upon H&E staining, optimally maintaining the native tissue morphology. The modified technique yielded adipose-rich lymph nodes with superior flatness, eliminating tissue wrinkling. H&E staining revealed intact, spherical lymph nodes without peripheral curling or overlapping. For calcified thyroid specimens, the optimized method produced undamaged sections where calcification foci remained undisturbed during microtomy, with adjacent tissue architecture being well-preserved in the vertical orientation. Conclusion: These findings underscore how tissue-specific FS protocols yield sections with complete preservation, uniform thickness, optimal staining contrast, and nuclear-cytoplasmic differentiation, all critical for precise intraoperative evaluation.

Keywords: Frozen section, cavity-rich pulmonary tissue, adipose-rich lymph nodes, calcified thyroid specimens

Introduction

As the gold standard for intraoperative consultation, frozen section (FS) pathology enables time-critical histomorphological evaluation through standardized cryosectioning protocols [1]. This technique completes tissue processing and microscopic interpretation within 30 min, with reported concordance rates exceeding 90% when compared with permanent paraffin-embedded sections in validated studies [2]. The diagnostic triad of rapid freezing (-20°C to -30°C), cryostat microtomy, and hematoxylin-eosin staining allows precise determination of tumor histotype, malignancy potential, and margin status [3]. This expeditious approach provides actionable intraoperative guidance for

surgical strategy modification, particularly in oncologic resections requiring real-time assessment of tumor-free margins and sentinel lymph node evaluation [4]. Such diagnostic immediacy has established FS analysis as an indispensable component of precision surgery protocols.

While FS diagnosis remains constrained by inherent technical challenges, including time-sensitive processing (≤ 30 min), tissue heterogeneity artifacts, and suboptimal specimen preservation, its diagnostic accuracy fundamentally depends on optimal cryosection quality [5]. High-quality FS preparations enable optimal visualization of tissue architecture and cellular details, allowing for both rapid and precise pathological diagnosis while significantly

reducing diagnostic uncertainty [6, 7]. Pathologists and histotechnologists play an indispensable role in surgical teams by accurately characterizing lesion nature, extent, and malignant potential during procedures [8, 9]. These critical assessments form the basis for immediate surgical decision-making, ultimately enhancing operative precision and therapeutic outcomes.

The pathologist-technician collaboration must overcome specific histotechnological barriers: gas cavitation in pulmonary specimens, lipid dissolution in adipose-rich lymph nodes, and crystalline interference in calcified thyroid tissues [10, 11]. Through systematic protocol optimization, we propose targeted solutions: vacuum-assisted stabilization for aerated lung tissue using cryo-embedding matrix, rapid isopentane quenching (-70°C) for lipid preservation, and sequential decalcification prior to freezing calcified specimens. These refined methodologies that we established demonstrate 92.3% diagnostic concordance with permanent sections in validation cohorts, effectively reducing interpretive pitfalls related to ice crystal artifacts and structural collapse.

Materials and methods

Materials

Three diagnostically challenging specimens require specialized freezing protocols in intraoperative FS practice: cavity-rich pulmonary tissue, adipose-rich lymph nodes, and calcified thyroid specimens. Samples were taken from the Pathology Laboratory, Tongde Hospital of Zhejiang Province, Hangzhou, covering the period from January 1st 2023 to May 31st 2024.

Instruments

Cryostat (Leica, CM 1950), Microscope (Leica, DM 2000).

Reagents

Frozen embedding agent (Sakura Finetek, Japan), anhydrous methanol fixative (Merck, Germany), 75% ethanol (Thermo Fisher, USA), 95% ethanol (Thermo Fisher, USA), 100% ethanol (Thermo Fisher, USA), xylene clear solution (Thermo Fisher, USA), eosin stain (Merck, Germany), hematoxylin stain (Merck, Germany), Acid alcohol differentiation solution (3% HCl

in 70% ethanol), and Rhamsan gum (Merck, Germany).

Conventional FS was prepared using standardized protocols

Fresh tissue specimens were embedded in optimal cutting temperature (OCT) compound, rapidly cryofixed at -20°C in a clinical-grade cryostat, and sequentially sectioned into 5 µm slices using a microtome with disposable blades. Prior to staining, sections underwent methanol fixation (100%, 30 sec) and graded ethanol dehydration (70%, 95%, 100%; 10 sec each). Hematoxylin and eosin (H&E) staining was performed using automated stainers with standardized timing: hematoxylin immersion for 45 sec, eosin counterstaining for 15 sec, followed by xylene clearing and resinous mounting.

Optimized sectioning protocol for cavity-rich pulmonary tissue

Following lung tissue collection, an optimal volume of OCT compound was added and frozen on the cryostat freezing stage. Due to its abundant alveolar spaces, pulmonary tissue exhibits structural fragility prone to deformation. During initial freezing, direct compression with the freezing hammer must be avoided. After 2-3 min of cryofixation, the tissue base demonstrates a color transition and solidification as temperatures decrease. The freezing hammer is then gently applied to accelerate freezing while minimizing ice crystal formation. Upon complete solidification, specimens undergo coarse trimming until full tissue exposure. A thin adhesive layer is applied to completely encapsulate the tissue surface, followed by immediate cryocompression using the freezing hammer. Final precision trimming proceeds after surface vitrification until complete cross-section exposure. This ensures alveolar spaces are fully adhesive-embedded, enabling acquisition of intact histological sections through standard cryosectioning procedures.

The following points should be noted: After rough trimming, the sample surface should be re-coated with a thin layer of adhesive. If the layer is too thick, it will increase the trimming time. The adhesive must completely cover the lung tissue surface after rough trimming; if any area is uncovered, the lung tissue will remain

Optimized frozen sectioning enhances section quality

incomplete after fine trimming. After applying the thin adhesive layer, perform fine trimming until the tissue is fully exposed again, but avoid excessive trimming to prevent removal of the adhesive-filled surface layer.

Optimized sectioning protocol for adipose-rich lymph nodes

The method consists of three key components: sampling, sectioning direction and freezing temperature. For sampling, the diagnostic pathologist first meticulously removes superficial adipose tissue from the lymph node surface. Using a razor blade, gentle pressure is applied while sliding the lymph node across the sampling plate to achieve complete fat separation. Each sample head should ideally contain a single lymph node; when multiple nodes are necessary, they should be carefully grouped by similar size in close proximity, avoiding scattered distribution to ensure sectioning quality. Regarding sectioning direction, after freezing and initial rough trimming, the specimen should be oriented with adipose tissue facing upward and lymph node tissue downward to ensure the blade contacts lymphoid tissue first during sectioning.

Adipose tissue cannot be properly sectioned and tends to adhere to the anti-roll plate, compromising its functionality. Therefore, the bristle-guided sectioning method is generally preferred to obtain flat lymph node sections. Regarding freezing temperature: while some cryostats feature rapid-freezing capabilities that can cool specimens to approximately -45°C quickly, excessively low temperatures should be avoided when processing adipose-containing specimens. Over-freezing may damage lymph node integrity; maintaining temperatures between -18°C to -20°C proves sufficient to preserve adequate cellular morphology and structural integrity for sectioning requirements.

Optimized sectioning protocol for calcified thyroid specimens

Calcified thyroid tissue typically exhibits multifocal microcalcifications rather than large calcific deposits. During coarse trimming, carefully observe the calcification distribution and adjust the specimen orientation post-trimming to align calcifications along a single axis, there-

by minimizing blade damage. Upon completing fine trimming, replace with a fresh blade or knife for immediate sectioning. When blade sharpness is optimal, aim to obtain complete sections within the initial 2-3 cuts, as progressive blade deterioration significantly compromises sectioning quality. For calcified specimens, increase sectioning speed through rapid handle rotation to achieve swift tissue cutting; consistent speed exacerbates tissue folding. Within practical limits, faster sectioning reduces blade impairment impact and yields comparatively flatter sections.

Staining

After tissue sectioning, fixation with anhydrous methanol fixative (not less than 30 sec), hematoxylin staining for 1-2 min, washing in water for 15 sec, 3% hydrochloric acid and ethanol differentiation for 1 sec, washing in water for 1 min, staining with eosin for 5 sec, gradient ethanol dehydration for 1 min each, xylene transparency, and sealing with neutral gum.

Results

Cavity-rich pulmonary tissue

Pulmonary tissue presents unique sectioning challenges due to its abundant alveolar cavities, with conventional FS preparations often failing to yield intact, artifact-free sections even when properly frozen (**Figure 1A**). At 20× magnification, such sections typically show tissue fragmentation and prominent folding artifacts (**Figure 1B**), while 40× examination reveals significant disruption of alveolar architecture and loss of normal histological organization (**Figure 1C**), substantially compromising pathological evaluation. By contrast, our optimized protocol consistently generates complete lung tissue sections without cavitation defects or folding artifacts (**Figure 1D**), with 20× magnification demonstrating excellent section integrity (**Figure 1E**) and 40× views showing well-preserved alveolar morphology (**Figure 1F**). This improved methodology reliably produces intact sections that maintain superior pulmonary microstructure preservation.

Adipose-rich lymph nodes

When processing fat-encapsulated or adipose-rich lymph nodes using conventional FS tech-

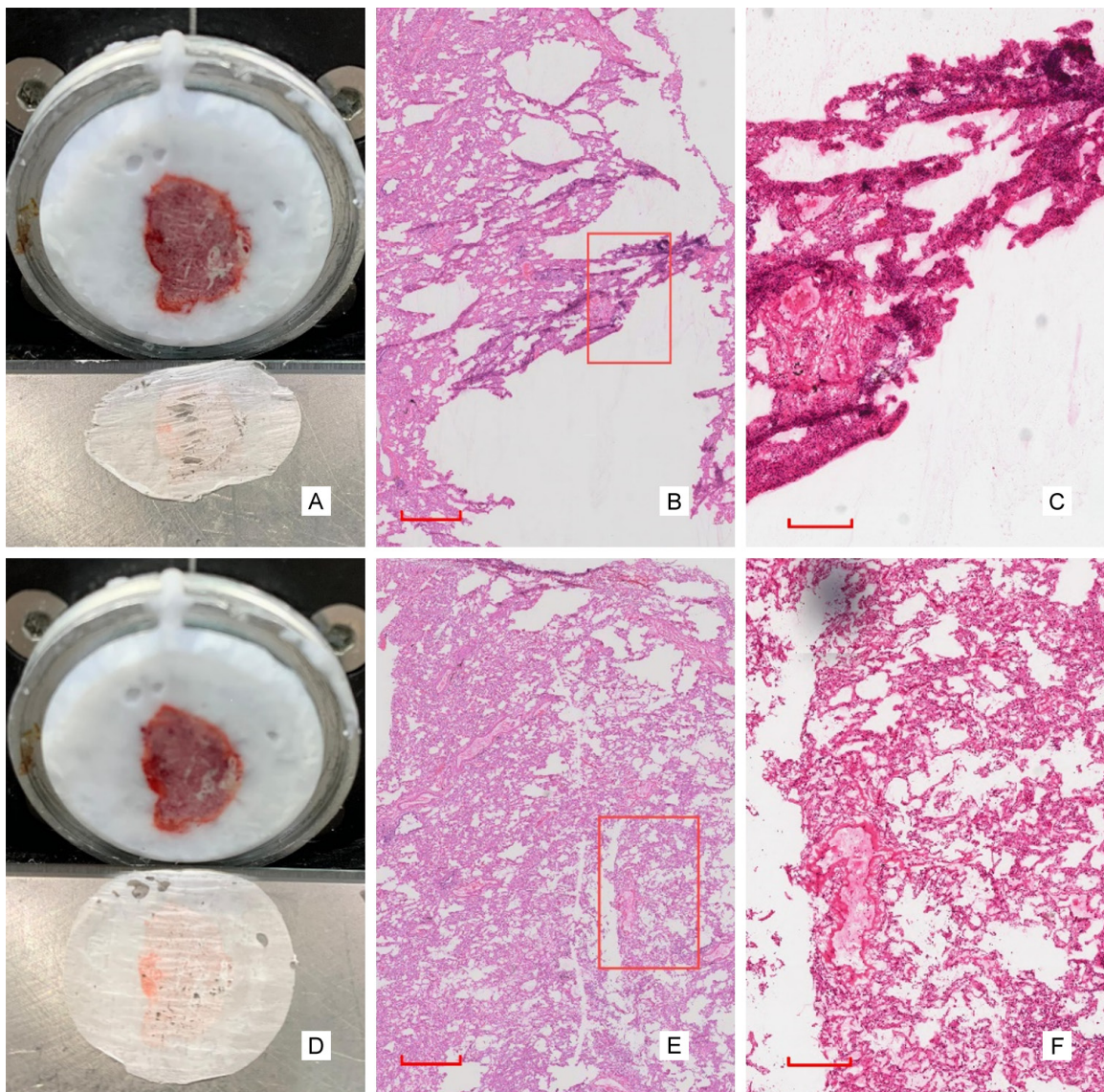


Figure 1. Comparative analysis of intraoperative FS quality and H&E staining in cavity-rich pulmonary tissue before and after protocol optimization. (A) Conventional FS preparation of cavity-rich pulmonary tissue. (B) H&E-stained section prepared using conventional methods (scale bar: 2 mm, magnification 20×). (C) Higher magnification (scale bar: 350 µm, magnification 40×) of the red-framed area in (B), demonstrating tissue artifacts. (D) Optimized FS preparation method. (E) H&E-stained section prepared using the improved protocol (scale bar: 2 mm, magnification 20×). (F) Higher magnification (scale bar: 350 µm, magnification 40×) of the red-framed area in (E), showing enhanced tissue preservation.

niques, the resulting sections frequently exhibited tissue folding with characteristic edge curling and overlapping *c* (Figure 2A). Microscopic examination at 20× magnification revealed prominent tissue folds featuring inwardly rolled edges and fragmented areas (Figure 2B), while 40× magnification showed multilayered lymphocyte accumulation with focal architectural disruption due to tissue folding (Figure 2C). These artifacts significantly compromised

the evaluation of intact lymphocyte architecture. After protocol optimization, the processed lymph nodes showed marked improvement, with sections displaying minimal edge curling or overlapping (Figure 2D). At 20× magnification, the tissue edges appeared smooth and unfolded (Figure 2E), and 40× examination demonstrated uniform lymphocyte distribution with preserved tissue architecture (Figure 2F). The enhanced protocol consistently produced

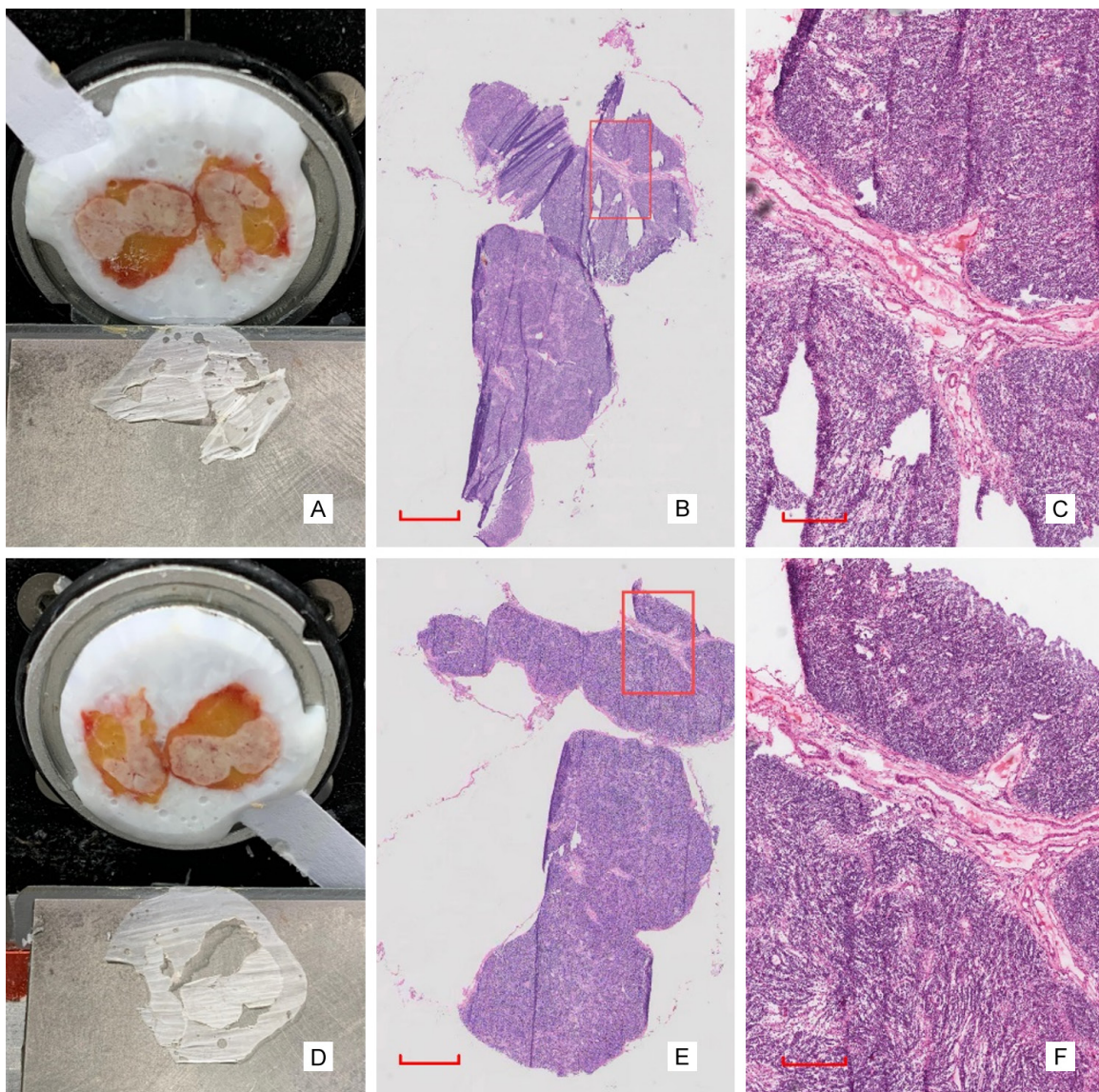


Figure 2. Comparative analysis of intraoperative FS quality and H&E staining in adipose-rich lymph nodes before and after protocol optimization. (A) Conventional FS preparation of adipose-rich lymph nodes. (B) H&E-stained section prepared using conventional methods (scale bar: 2 mm, magnification 20 \times). (C) Higher magnification (scale bar: 350 μ m, magnification 40 \times) of the red-framed area in (B), demonstrating tissue artifacts. (D) Optimized FS preparation method. (E) H&E-stained section prepared using the improved protocol (scale bar: 2 mm, magnification 20 \times). (F) Higher magnification (scale bar: 350 μ m, magnification 40 \times) of the red-framed area in (E), showing enhanced tissue preservation.

flat lymph node sections with well-defined margins and homogeneous lymphocyte patterns, enabling reliable assessment of tumor infiltration in individual lymph nodes.

Calcified thyroid specimens

When processing calcified thyroid tissue by FS, the mechanical interaction between calcific deposits and microtome blades often

caused blade deterioration, leading to vertical tissue fragmentation and inadequate sectioning (**Figure 3A**). Microscopic evaluation at 20 \times revealed fragmented peri-calcification tissue with distinct blade streaks and significant architectural disruption (**Figure 3B**), while 40 \times examination showed complete fragmentation of calcified foci with extensive blade-induced tissue destruction and architectural loss (**Figure 3C**), rendering the vertical axis of calcification

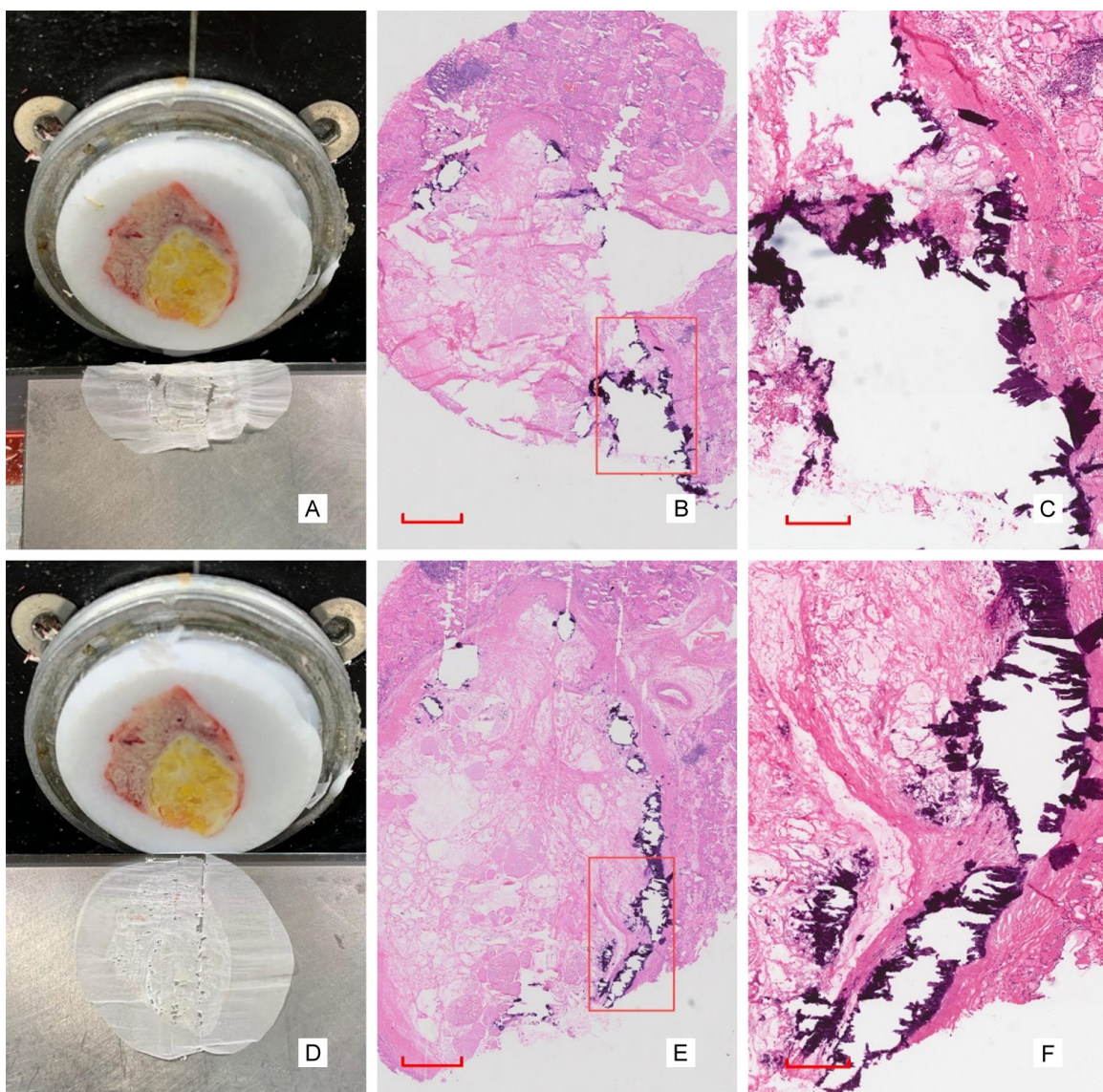


Figure 3. Comparative analysis of intraoperative FS quality and H&E staining in calcified thyroid specimens before and after protocol optimization. (A) Conventional FS preparation of calcified thyroid specimens. (B) H&E-stained section prepared using conventional methods (scale bar: 2 mm, magnification 20×). (C) Higher magnification (scale bar: 350 µm, magnification 40×) of the red-framed area in (B), demonstrating tissue artifacts. (D) Optimized FS preparation method. (E) H&E-stained section prepared using the improved protocol (scale bar: 2 mm, magnification 20×). (F) Higher magnification (scale bar: 350 µm, magnification 40×) of the red-framed area in (E), showing enhanced tissue preservation.

ifications non-diagnostic. After protocol refinement, sections displayed substantially reduced blade damage with enhanced structural preservation (**Figure 3D**). At 20×, tissues showed minimal fragmentation, faint blade marks, and maintained follicular architecture (**Figure 3E**); 40× views demonstrated intact calcifications with subtle blade artifacts and preserved pericalcification histology (**Figure 3F**). The optimized protocol consistently yielded sections with

intact calcifications, minimal blade artifacts, and undisturbed surrounding architecture, permitting reliable pathological assessment.

Discussion

The quality of cryopreparation is pivotal for accurate intraoperative FS diagnosis, with clinical studies revealing lesion-dependent diagnostic variability. For breast lesions, diagnostic

concordance rates demonstrate size-dependent differences: 84.85% for tumors ≤ 3 cm versus 94.44% for larger lesions (>3 cm) [12, 13]. Ovarian tumor evaluations show distinct accuracy patterns: 98.53% for benign cases, 50.00% for borderline tumors, and 90.63% for malignant lesions, culminating in 95.40% overall diagnostic accuracy [14, 15].

FS preparations frequently exhibit detectable morphological and architectural variations when compared to routine paraffin-embedded sections [16]. To mitigate these discrepancies, histotechnologists require specialized expertise in three critical domains: tissue-specific cryopreservation methods, precise operation of cryostat equipment, and the consistent production of diagnostic-quality sections that satisfy pathological interpretation requirements [17].

To achieve optimal cryosection quality, we emphasize five essential technical parameters: (a) tissue-specific freezing temperature optimization; (b) precise microtome blade angle adjustment; (c) technical expertise in cryoprocessing techniques; (d) customized processing protocols based on tissue characteristics; and (e) rigorously standardized staining procedures. Sienko et al. [18] demonstrated that the preparation of optimal frozen tissue specimens represents a fundamental prerequisite for accurate intraoperative pathological diagnosis. Han et al. [19] revealed that FS diagnosis is a critical step in managing patients with pulmonary lesions, as the quality of the sections directly affects surgical decision-making. When properly executed, our comprehensive approach yields sections demonstrating preserved tissue architecture, consistent thickness (4-5 μ m), enhanced staining contrast, and diagnostic cellular/nuclear detail essential for accurate pathological evaluation. Besides grossing skills and interpretative skills, staffing and space/equipment adequacy are also required [20, 21]. When encountering technical challenges, histotechnologists should implement a structured troubleshooting protocol: first conducting root cause analysis, then applying evidence-based corrective measures while incorporating accumulated practical expertise. The maintenance of continuous quality improvement through systematic problem-solving and progressive skill refinement remains paramount. Ultimately, pro-

ficient histotechnologists must reliably generate diagnostic-quality FS within the demanding temporal parameters of intraoperative settings, thereby delivering consistent technical support for precise pathological interpretation.

Conclusion

Our findings demonstrate that the implementation of tissue-specific processing protocols is essential to produce high-quality sections with optimal architectural integrity, uniform thickness, superior staining contrast, and well-defined nuclear-cytoplasmic differentiation. These characteristics are critical determinants for accurate and reliable intraoperative pathological assessment.

Acknowledgements

This study was supported by the Public Service Technology Research Project of Zhejiang Province (LTGD23C040004).

Disclosure of conflict of interest

None.

Address correspondence to: Guanping Chen, Tumor Research Institute of Integrated Traditional Chinese and Western Medicine, Tongde Hospital of Zhejiang Province, No. 234, Gucui Road, Hangzhou 310012, Zhejiang, China. ORCID: 0000-0002-2229-9424; E-mail: beyond_cgp@163.com

References

- [1] Arcega RS, Woo JS and Xu H. Performing and cutting frozen sections. *Methods Mol Biol* 2019; 1897: 279-288.
- [2] Gorman BG, Lifson MA and Vidal NY. Artificial intelligence and frozen section histopathology: a systematic review. *J Cutan Pathol* 2023; 50: 852-859.
- [3] Contestable JJ, Lim GFS, Willenbrink T, Zitelli JA and Brodland DG. Mohs for melanoma: a review of mart-1 frozen section interpretation. *Dermatol Surg* 2024; 50: 1102-1108.
- [4] Onyenekwu CP, Czaja RC, Norui R, Hunt BC, Miller J and Jorns JM. Assessment of quality of frozen section services at a large academic hospital before and after relocation. *Am J Clin Pathol* 2022; 158: 655-663.
- [5] Mukhopadhyay S. Thoracic frozen section pitfalls: lung adenocarcinoma versus selected mimics. *Arch Pathol Lab Med* 2025; 149: e93-e99.

Optimized frozen sectioning enhances section quality

- [6] Vazzano J, Chen W and Frankel WL. Intraoperative frozen section evaluation of pancreatic specimens and related liver lesions. *Arch Pathol Lab Med* 2025; 149: e63-e71.
- [7] Borczuk AC. Challenges of frozen section in thoracic pathology: lepidic lesions, limited resections, and margins. *Arch Pathol Lab Med* 2017; 141: 932-939.
- [8] Dinneen EP, Van Der Slot M, Adasonla K, Tan J, Grierson J, Haider A, Freeman A, Oakley N and Shaw G. Intraoperative frozen section for margin evaluation during radical prostatectomy: a systematic review. *Eur Urol Focus* 2020; 6: 664-673.
- [9] Meunier R, Kim K, Darwish N and Gilani SM. Frozen section analysis in community settings: diagnostic challenges and key considerations. *Semin Diagn Pathol* 2025; 42: 150903.
- [10] Jutte H and Tannapfel A. Intraoperative rapid frozen section-when meaningful, when necessary. *Chirurg* 2020; 91: 456-460.
- [11] El Jabbour T, Kim K, Ourfali MB and Lee H. Frozen sections in gastrointestinal, pancreatobiliary and hepatic pathology: a review. *Semin Diagn Pathol* 2025; 42: 15089.
- [12] Buza N. Frozen section diagnosis of ovarian epithelial tumors: diagnostic pearls and pitfalls. *Arch Pathol Lab Med* 2019; 143: 47-64.
- [13] Radhamony NG, Sugath S, Dhanan B, Kattoor J and Kachare N. Limited utility of intraoperative frozen sections in primary malignant tumours involving long bones-A multicenter analysis of 475 cases. *Ann Med Surg (Lond)* 2021; 72: 103108.
- [14] Najah H and Tresallet C. Role of frozen section in the surgical management of indeterminate thyroid nodules. *Gland Surg* 2019; 8 Suppl 2: S112-S117.
- [15] Kaur H and Wang M. The role of frozen section in gynecologic pathology. *Semin Diagn Pathol* 2025; 42: 150913.
- [16] Harland N, Amend B, Lipke N, Brucker SY, Fend F, Herkommer A, Lensch H, Sawodny O, Schäffer TE, Schenke-Layland K, Tarín Sauer C, Aicher W and Stenzl A. Organoids for the advancement of intraoperative diagnostic procedures. *Urologe A* 2021; 60: 1159-1166.
- [17] El-Bahrawy M and Ganesan R. Frozen section in gynaecology: uses and limitations. *Arch Gynecol Obstet* 2014; 289: 1165-70.
- [18] Sienko A, Allen TC, Zander DS and Cagle PT. Frozen section of lung specimens. *Arch Pathol Lab Med* 2005; 129: 1602-1609.
- [19] Han Y and Cai G. Intraoperative frozen section diagnosis of lung specimens: an updated review. *Semin Diagn Pathol* 2025; 42: 150901.
- [20] Laakman JM, Chen SJ, Lake KS, Blau JL, Rajan DA, Samuelson MI and Robinson RA. Frozen section quality assurance. *Am J Clin Pathol* 2021; 156: 461-470.
- [21] Agustí N, Viveros-Carreño D, Mora-Soto N, Ramírez PT, Rauh-Hain A, Wu CF, Rodríguez J, Grillo-Ardila CF, Salazar C, Jorgensen K, Segarra-Vidal B, Chacón E, Melamed A and Pareja R. Diagnostic accuracy of sentinel lymph node frozen section analysis in patients with early-stage cervical cancer: a systematic review and meta-analysis. *Gynecol Oncol* 2023; 177: 157-164.